Proceedings of the International Conference on Industrial Engineering and Operations Management
Bandung, Indonesia, March 6-8, 2018

Discrete Wavelet Packet Based Spectrum Sensing in Cognitive Radio using an Improved Adaptive Threshold

Dibal Peter Yusuf, Elizabeth Onwuka, and Caroline, Alenoghena
Telecommunications Engineering Department, Federal University of Technology Minna
James Agajo
Computer Engineering Department, Federal University of Technology Minna

Abstract

Thresholding is a very important technique in the detection of spectrum holes in cognitive radios. It is the benchmark by which a cognitive radio decides if a spectrum hole is present or not in a given frequency spectrum. However, the method by which a cognitive radio computes the threshold for any given scenario can be quite a challenge in terms of accuracy, speed, and efficiency. Fixed thresholds are less cumbersome to implement, but they are characterized by undesirable sensitivity and performance issues in the radio environment in which the cognitive radio operates due to uncertainty in noise level. On the other hand, adaptive thresholds give superior performance to fixed thresholds due to their ability to adjust their computational parameters in response to changes in the cognitive radio environment. In this paper, we present a discrete wavelet packet transform (DWPT) based spectrum sensing in cognitive radio with an improved adaptive threshold in terms of speed. The approach developed in this paper halves the number of computations needed to determine the adaptive threshold for each sub-band channel in a discrete wavelet packet transform. The results obtained show the method is efficient, fast, and dynamic in response to the variations in the cognitive radio environment.

Keywords: Cognitive Radio; Optimization; Adaptive threshold; noise uncertainty, DWPT

1.0 Introduction

The electromagnetic spectrum is a unique natural resource which is at the core of the operation of wireless technology and devices. It is a resource that is reusable by wireless transceiver systems which are licensed by government agencies based on certain conditions and criteria. Like any other natural resource, the electromagnetic spectrum is certainly finite. This limitation poses a great challenge in the presence of the ever-increasing wireless devices and applications which place a high demand on the available electromagnetic spectrum [1]. One candidate solution in literature is the cognitive radio (CR) technology which operates through a cognitive cycle [2-4] shown in Figure 1[2] in order to mitigate this problem. The cognitive radio cycle consists of three major components:

i. Radio scene analysis which encompasses radio environment interference temperature estimation, and spectrum hole detection.

ii. Channel identification which encompasses estimation of information about channel space, and channel capacity prediction.

iii. Dynamic spectrum management, and control of transmit power.

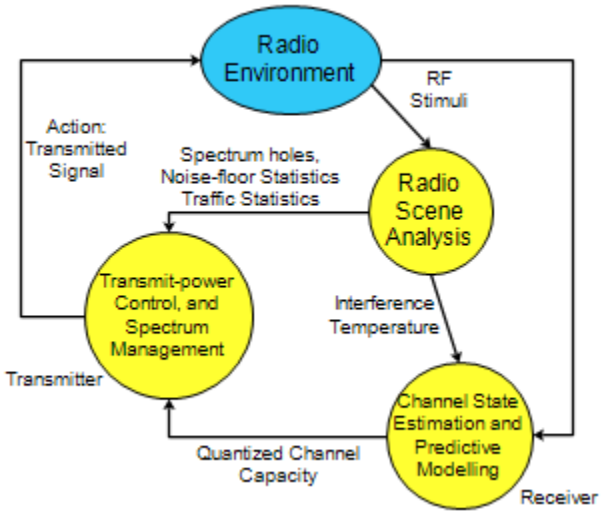

Figure 1: Cognitive Radio Cycle

This paper focuses on the radio scene analysis stage of the cognitive radio cycle in which we achieve detection of spectrum holes through spectrum sensing function. At the heart of spectrum hole detection is the technique of thresholding. Thresholds could be either fixed or adaptive. Fixed thresholds have the disadvantage of poor spectrum management in the presence of varying radio environment characteristics. Adaptive thresholds ensure efficient and accurate detection of spectrum holes as the characteristics of the radio environment changes. The improved adaptive threshold presented here is based on the discrete wavelet packet transform (DWPT), and has the ability to resolve signals in both time and frequency [5-9]. However, it should be pointed out that regardless of how well an adaptive threshold is designed, the performance of the spectrum sensing scheme implementing it will always be affected by noise uncertainty [10-11].

2.0 Effect of Noise Uncertainty in Adaptive Thresholding

Noise in communication systems occur as a result of the aggregation of random sources of electromagnetic (EM) energy, which includes thermal noise and interference. Unintended emissions, and weak signals caused by large distances between transmitters and receivers are typical examples of random EM energy sources. From the foregoing, noise uncertainty can be described as a phenomenon brought about by random variations in noise level, and it causes degradation in the performance of most spectrum sensing schemes in terms of accuracy, if the signal-to-noise (SNR) is low [11-12].

When noise uncertainty occurs, the variance of the noise distributes within the range of $\left[\alpha\sigma_n^2, \frac{1}{\alpha}\sigma_n^2\right]$ [12-13]. Thus, an estimated noise power can be expressed as:

$$\hat{\sigma}_n^2 = \alpha\sigma_n^2 \tag{1}$$

where α is a noise uncertainty interval and σ_n^2 is a noise variance.

It can be seen from the foregoing that due to noise uncertainty, adaptive thresholds remain very important in order to maintain an acceptable level of accuracy by a spectrum sensing scheme in the presence of such variations. An adaptive threshold will typically update itself by taking noise uncertainty and SNR into consideration, thus ensuring an optimum response in the spectrum sensing process.

Another important factor is the type of the transform used in the spectrum sensing algorithm; it is here that wavelets outperform other transforms owing to their ability to effect time-frequency resolution of signals [5-9]. Typically, wavelets mitigate the effects of noise uncertainty through the selection of best basis function which ensures minimal representation of the data relative to the cost function. The selection of the best basis ensures that Gaussian noise remains Gaussian after the wavelet transform. This assertion is possible because higher order wavelet moments like skewness and kurtosis for Gaussian processes have theoretical values of zero [11,14].

3.0 Discrete Wavelet Packet Transform (DWPT) Threshold Improvement

Wavelets are extensively applied in the analysis of data; they are powerful tools that are used in the representation of both known and unknown signals as a set of functions with the sole aim of gaining better insight into their characteristics. The discrete wavelet packet transform as shown in Figure 2 [9] is a generalization of wavelet transform in which a tree structure is used in the implementation of the wavelet algorithm by decomposing an input signal through high-pass and low-pass filter branches [15-18].

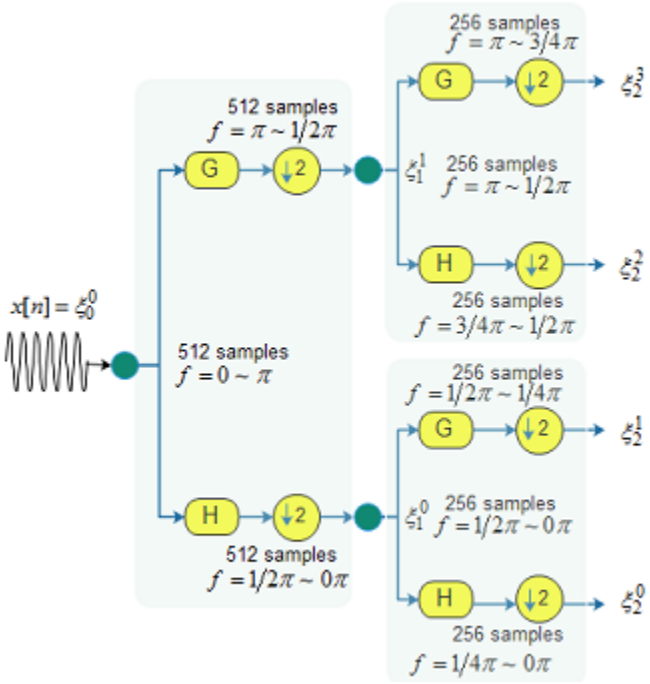

Fig 2: Analysis filter bank of a wavelet packet

For the wavelet packet tree shown in Figure 2, the wavelet packet coefficients $\xi_{l+1}^{2p}[n]$ are generated using the scaling filter. Similarly, the coefficients $\xi_{l+1}^{2p+1}[n]$ are generated using the wavelet filter. Mathematically, the coefficients are expressed as [9]:

$$\xi_{l+1}^{2p}[n] = \sqrt{2}\sum_{k} h[k]\xi_{l}^{p}[2n-k], n = 0,1,..., N-1 \tag{2}$$

$$\xi_{l+1}^{2p+1}[n] = \sqrt{2}\sum_{k} g[k]\xi_{l}^{p}[2n-k], n = 0,1,2,..., N-1 \tag{3}$$

where $h[k]$ is the low-pass filter, $g[k]$ is the high-pass filter, and p is the position at level l.

For the signal in each sub-band channel, the energy is calculated as [19-20]:

$$E = \frac{1}{T}\int_{0}^{T}\left[\sum_{j\geq j_0}\sum_{k} c_{j,k}\phi_{j,k}(t) + d_{j,k}\psi_{j,k}\right]^2 dt \tag{4}$$

$$E = \frac{1}{T}\sum_{j\geq j_0}\sum_{k}\left(c_{j,k}^2 + d_{j,k}^2\right) \tag{5}$$

where $c_{j,k}$ is scaling function coefficient, $d_{j,k}$ is the wavelet function coefficient. It should be noted that the presence of a signal in a sub-band channel makes the energy level of that signal in the sub-band channel higher.

In this paper we focus on the improvement of the thresholding by Q. Zhijin, et al in [19] which we will call the referred scheme and given as:

$$\lambda_{i+1,2j} = \frac{\lambda_{i,j} + \alpha E_{i+1,2j}}{2} \tag{6}$$

$$\lambda_{i+1,2j-1} = \frac{\lambda_{i,j} + \alpha E_{i+1,2j-1}}{2} \tag{7}$$

The expressions in (6) and (7) yield the adaptive threshold at channel j during the *(i+1)th* level of decomposition. To better understand these equations, we present in Figure 3, the relationship in a DWPT between a parent node and the two child nodes that originate from it.

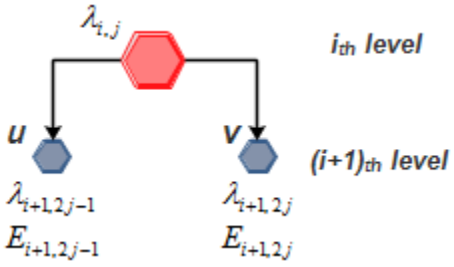

Figure 3: Relationship between a parent node and child nodes in a DWPT

As seen in Figure 3, $\lambda_{i,j}$ is the threshold associated with the parent node, while $\lambda_{i+1,2j}$ and $\lambda_{i+1,2j-1}$ are the thresholds associated with the two child nodes *u* and *v* at the *(i+1)th* level of DWPT decomposition. $E_{i+1,2j}$ and $E_{i+1,2j-1}$ are the energies associated with the two child nodes *u* and *v* at the *(i+1)th* level of DWPT decomposition. The factor α is a tuning factor in the determination of the adaptive threshold, and as it tends to 1, the energy of the received signal has a profound effect on the adaptive threshold; if it tends to zero, the threshold at *(i+1)th* level becomes half the threshold at the *ith* level.

To make an improvement on this threshold determination technique, we explore the norm of the Euclidean distance between the two child nodes *u* and *v* in Figure 3, and compute the energy associated with this distance. We refer to this approach as the proposed scheme.

Each node in the DWPT shown in Figures 2 and 3 can be viewed as a vector in a vector field $\mathbb{F}$. Thus, child node *u* can be viewed as a vector $\mathbf{u}$ with components $\begin{bmatrix} u_1 & u_2 & \cdots \end{bmatrix}$. In the same manner, child node *v* can be viewed as a vector $\mathbf{v}$ with components $\begin{bmatrix} v_1 & v_2 & \cdots \end{bmatrix}$.

Let us define a vector $\mathbf{w}$ to be the Euclidean distance between $\mathbf{u}$ and $\mathbf{v}$. $\mathbf{w}$ can be expressed as [21-24]:

$$\mathbf{w}(\mathbf{u},\mathbf{v}) = \left[(\mathbf{u}-\mathbf{v})^{\mathrm{T}} (\mathbf{u}-\mathbf{v}) \right]^{\frac{1}{2}} \tag{8}$$

where the expression $(\mathbf{u}-\mathbf{v}) = \begin{bmatrix} u_1 \\ u_2 \\ \vdots \\ u_n \end{bmatrix} \begin{bmatrix} v_1 \\ v_2 \\ \vdots \\ v_n \end{bmatrix}$. The norm of the Euclidean distance in (8) is:

$$\left\| \mathbf{w}(\mathbf{u},\mathbf{v}) \right\|_2 = \left\| \mathbf{w} \right\|_2 = \left\| \left[(\mathbf{u}-\mathbf{v})^{\mathrm{T}} (\mathbf{u}-\mathbf{v}) \right]^{\frac{1}{2}} \right\|_2 \tag{9}$$

The vector $\mathbf{w}$ is influenced by both vectors $\mathbf{u}$ and $\mathbf{v}$. Hence, it can be used to benchmark either $\mathbf{u}$ or $\mathbf{v}$. Using (5), the energy in the vector $\mathbf{u}$ can be expressed as:

$$E_{i+1,2j-1} = E_{\mathbf{u}} = \frac{1}{T}\sum_{j\geq j_0}\sum_{k}\left(c_{j,k}^2 + d_{j,k}^2\right)_{i+1,2j-1} \tag{10}$$

and the energy in $\mathbf{v}$ can be expressed as:

$$E_{i+1,2j} = E_{\mathbf{v}} = \frac{1}{T}\sum_{j\geq j_0}\sum_{k}\left(c_{j,k}^2 + d_{j,k}^2\right)_{i+1,2j} \tag{11}$$

Applying (8) to (10) and (11), we can express the energy in the vector $\mathbf{w}$ in terms of the energy in vectors $\mathbf{u}$ and $\mathbf{v}$ as:

$$E_{\mathbf{w}}\left(E_{\mathbf{u}},E_{\mathbf{v}}\right) = E_{\mathbf{w}}\left(E_{i+1,2j-1},E_{i+1,2j}\right) = \left[\left(\frac{1}{T}\sum_{j\geq j_0}\sum_{k}\left(c_{j,k}^2 + d_{j,k}^2\right)_{i+1,2j-1} - \frac{1}{T}\sum_{j\geq j_0}\sum_{k}\left(c_{j,k}^2 + d_{j,k}^2\right)_{i+1,2j}\right)^T\left(\frac{1}{T}\sum_{j\geq j_0}\sum_{k}\left(c_{j,k}^2 + d_{j,k}^2\right)_{i+1,2j-1} - \frac{1}{T}\sum_{j\geq j_0}\sum_{k}\left(c_{j,k}^2 + d_{j,k}^2\right)_{i+1,2j}\right)\right]^{\frac{1}{2}} \tag{12}$$

Factoring $1/T$ and the summation operator in (12) yields:

$$E_{\mathbf{w}}\left(E_{\mathbf{u}},E_{\mathbf{v}}\right) = E_{\mathbf{w}}\left(E_{i+1,2j-1},E_{i+1,2j}\right) = \frac{1}{T}\left\{\sum_{j\geq j_0}\sum_{k}\left[\left(\left(c_{j,k}^2 + d_{j,k}^2\right)_{i+1,2j-1} - \left(c_{j,k}^2 + d_{j,k}^2\right)_{i+1,2j}\right)^T\left(\left(c_{j,k}^2 + d_{j,k}^2\right)_{i+1,2j-1} - \left(c_{j,k}^2 + d_{j,k}^2\right)_{i+1,2j}\right)\right]\right\}^{\frac{1}{2}} \tag{13}$$

The expression in (13) is the energy of the Euclidean distance between vectors $\mathbf{u}$ and $\mathbf{v}$. Using (9), the norm of this energy is:

$$E_{\mathbf{w}}\left(E_{\mathbf{u}},E_{\mathbf{v}}\right) = \left\|\frac{1}{T}\left\{\sum_{j\geq j_0}\sum_{k}\left[\left(\left(c_{j,k}^2 + d_{j,k}^2\right)_{i+1,2j-1} - \left(c_{j,k}^2 + d_{j,k}^2\right)_{i+1,2j}\right)^T\left(\left(c_{j,k}^2 + d_{j,k}^2\right)_{i+1,2j-1} - \left(c_{j,k}^2 + d_{j,k}^2\right)_{i+1,2j}\right)\right]\right\}^{\frac{1}{2}}\right\|_2 \tag{14}$$

The effect of (14) is that rather than using two separate expressions to obtain the thresholds associated with two child nodes *u* and *v* which originate from the same parent node as in (6) and (7), we simply calculate the threshold for the two child nodes using one expression. The energy used in this singular expression for the calculation of the threshold is the energy of the vector which is derived from the Euclidean distance between the two child nodes. This approach reduces by half, the number of required computations for thresholding at any level of decomposition for the DWPT.

The implication of spectrum sensing with the proposed scheme is that the speed in increased because of the reduced number of computations. For example, consider the DWPT tree shown in Figure 4 which has 5 levels of decomposition under consideration in this paper. Using the referred scheme, 32 calculations will have to be made for the child nodes as level 5 because they are 32 in number. However, using the proposed scheme, only 16 calculations will have to be made for the child nodes at level 5 because of the utilization of the vector of the Euclidean distance (shown in red) between the child nodes at the level under consideration.

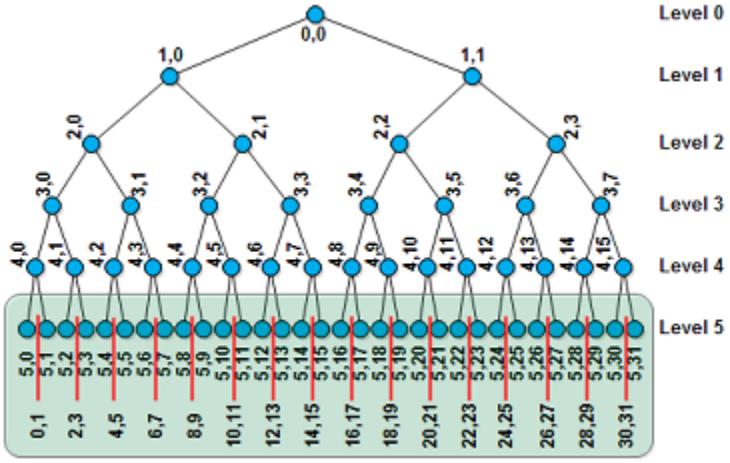

Figure 4: DWPT Tree at Level-5 Decomposition

By minimizing the expression in (14), we obtain an optimum value for $E_{\mathbf{w}}$ as $E_{\mathbf{w}}^{*}\left(E_{\mathbf{u}},E_{\mathbf{v}}\right)=\min E_{\mathbf{w}}\left(E_{\mathbf{u}},E_{\mathbf{v}}\right)$. Hence, the optimum value for (14) can be expressed as:

$$E_{\mathbf{w}}^{*}\left(E_{\mathbf{u}},E_{\mathbf{v}}\right)=\min\left\|\frac{1}{T}\left\{\sum_{j\geq j_0}\sum_{k}\left[\left(\left(c_{j,k}^{2}+d_{j,k}^{2}\right)_{i+1,2j-1}-\left(c_{j,k}^{2}+d_{j,k}^{2}\right)_{i+1,2j}\right)^{T}\left(\left(c_{j,k}^{2}+d_{j,k}^{2}\right)_{i+1,2j-1}-\left(c_{j,k}^{2}+d_{j,k}^{2}\right)_{i+1,2j}\right)\right]\right\}^{\frac{1}{2}}\right\|_{2} \tag{15}$$

From the foregoing therefore, the adaptive threshold at any level of decomposition using the proposed scheme is:

$$\lambda_{i+1,2j},\lambda_{i+1,2j-1}=\frac{\lambda_{i,j}+\alpha.\min\left\|\frac{1}{T}\left\{\sum_{j\geq j_0}\sum_{k}\left[\left(\left(c_{j,k}^{2}+d_{j,k}^{2}\right)_{i+1,2j-1}-\left(c_{j,k}^{2}+d_{j,k}^{2}\right)_{i+1,2j}\right)^{T}\left(\left(c_{j,k}^{2}+d_{j,k}^{2}\right)_{i+1,2j-1}-\left(c_{j,k}^{2}+d_{j,k}^{2}\right)_{i+1,2j}\right)\right]\right\}^{\frac{1}{2}}\right\|_{2}}{2} \tag{16}$$

4.0 Simulation and Results

The performance of the adaptive threshold technique was evaluated by simulation. The simulation involves a composite signal having different amplitudes and frequencies as described in Table 1, and varying SNR from -10dB to 10dB.

Table 1: Input Signal Parameters

	Amplitude	**Frequency (MHz)**
Signal 1	1.3	15
Signal 2	1.7	40
Signal 3	2.0	67
Signal 4	1.8	81

At -10dB, the input signal to the system is shown graphically in Figure 5.

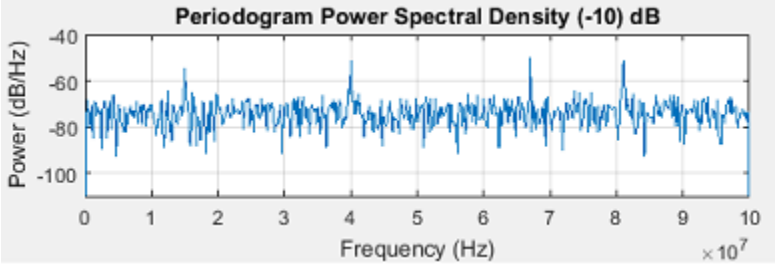

Figure 5: Input PSD at -10dB

The absolute value of the coefficients at -10dB in each sub-band channel at level-5 decomposition of the DWPT tree of Figure 4 is shown in Figure 6. The sub-band channels with higher energy value have coefficients with higher values. This assertion holds true because the energy in each sub-band channel is a function of the coefficients in that sub-band channel, as indicated by (5).

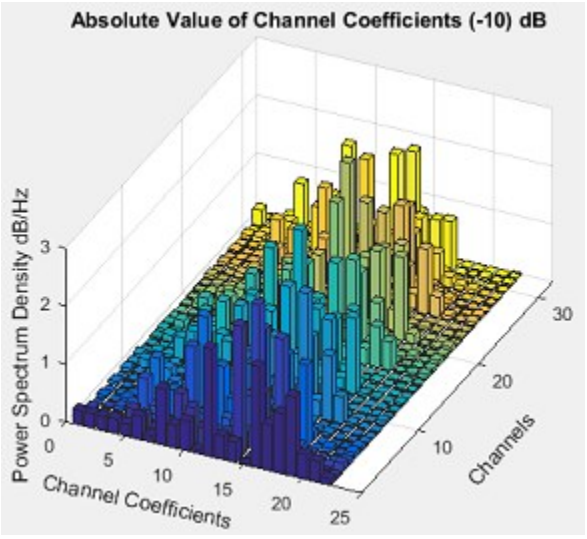

Figure 6: Distribution of coefficients in sub-band channels at -10dB

Using (15), we perform a simulation to obtain 16 Euclidean distance vectors between the 32 sub-band channels of Figure 4. The Euclidean distance vectors are shown in Figure 7.

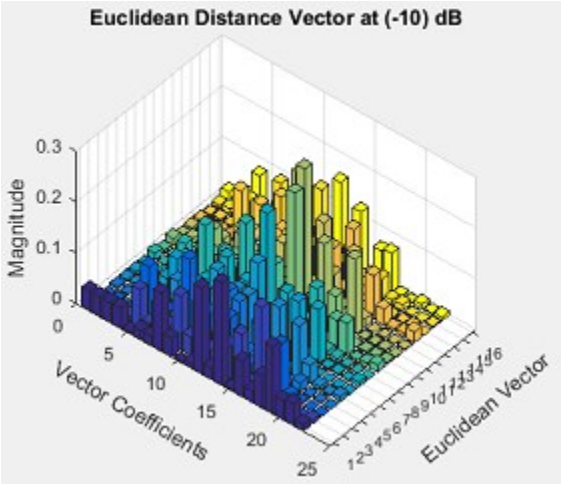

Figure 7: Euclidean vectors generated from DWPT sub-band channels

The optimization of the Euclidean distance vector by (16) yields a more compact vector field as shown in Figure 8.

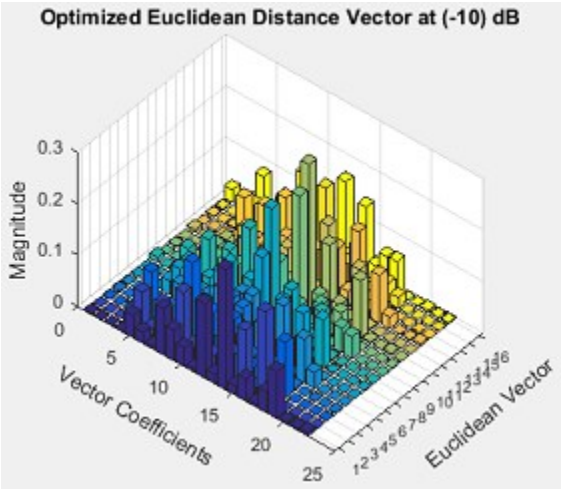

Figure 8: Optimized Euclidean vectors generated from DWPT sub-band channels

We perform spectrum sensing at signal-to-noise (SNR) values of -10dB, 0dB, and 10dB. The simulation result for spectrum sensing at -10dB is shown in Figure 9.

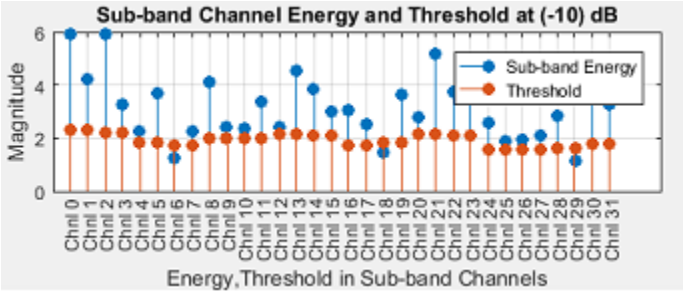

Figure 9: Comparison of sub-band threshold and energy at -10dB

At -10dB in Figure 9, sub-band channels 6, 18, and 29 were identified as UNOCCUPIED channels because the energy in those channels is less than the adaptive thresholds associated with the respective channels.

The SNR value was changed to 0dB, and upon simulation, the result obtained is shown in Figure 10.

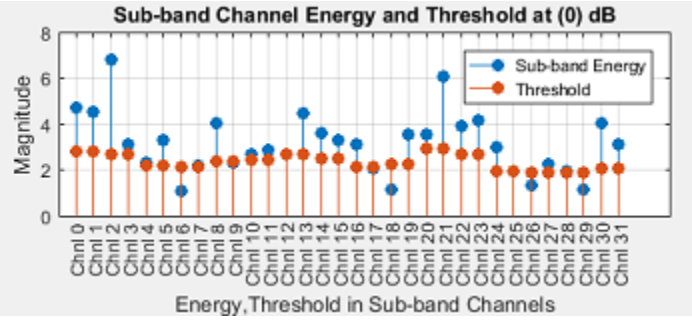

Figure 10: Comparison of sub-band threshold and energy at 0dB

At the SNR value of 0dB, six sub-band channels were identified as UNOCCUPIED. These include: 6, 9, 17, 18, 26, 29. Comparison of Figure 9, and 10, reveals that false alarms occurred in sub-band channels 9, 17, and 26 when the SNR value was set at -10dB. The false alarm occurred at -10dB because the noise was equal to the signal in strength due to the low value of the signal; hence, a detection technique can easily classify a noisy channel as OCCUPIED (which is a false alarm). However, as the SNR value increases, the signal strength increases, thus making a detection technique more accurate in detection and classification of sub-band channels.

The performance of this technique at 10dB is shown in Figure 11. At this value of SNR, ten sub-band channels were classified as UNOCCUPIED. The channels include: 6, 7, 9, 10, 12, 17, 18, 25, 26, and 29. It can be seen that there were false alarms for sub-band channels 7, 10, and 12 for the preceding values of the SNR.

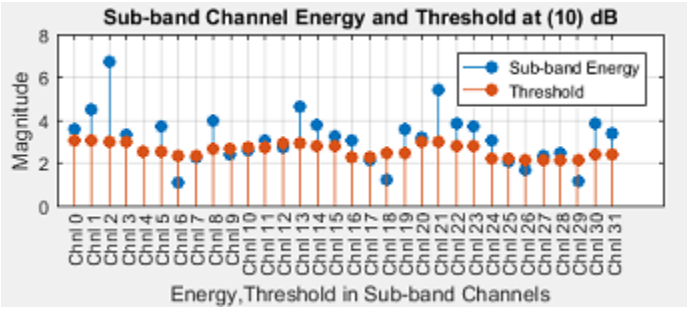

Figure 17: Comparison of sub-band threshold and energy at 5dB

From the foregoing analysis, it can be seen that the accuracy of the detector using the proposed adaptive thresholding technique increased with the increase in SNR value. Thus, the detector was able to make a better decision on the status of the DWPT sub-bands because of the increase in signal power. A summary of the performance of the detection with respect to increase in SNR is shown in Table 2.

Table 2: Performance of spectrum sensing technique for varying signal-to-noise ratios

SNR (dB)	Sub-band Channels Classified as UNOCCUPIED												Total Count
-10		6	18	29									3
0		6	9	17	18	26	29						6
10		6	7	9	10	12	17	18	25	26	29		10

6.0 Conclusion

In this paper, we explored the norm of the Euclidean distance between two vectors that characterize the terminal sub-bands of the DWPT. This vector was used as the basis for the improvement of a DWPT thresholding technique. The improvement achieved was in terms of speed of calculation required to compute the adaptive threshold for all sub-band channels at a given level of decomposition. The results and analysis of this approach showed that the accuracy of the proposed scheme with respect to increase in SNR was as expected.

Acknowledgement

We acknowledge the funding support we got from Tertiary Education Trust Fund (TETFund) with grant number: TETFUND/FUTMINNA/2017/B/04.

References

[1]. Cisco Visual Networking Index: Global Mobile Data Traffic Forecast Update 2015 – 2020. Online. Available at: [http://www.cisco.com/c/en/us/solutions/collateral/service-provider/visual-networking-index-vni/mobile-white-paper-c11-520862.html]. Accessed:27/03/2017

[2]. Haykin, S., Cognitive Radio: Brain-Empowered Wireless Communications, *IEEE Journal on Selected Areas in Communication*, vol. 23, no.2, pp. 201 – 220, 2015.

[3]. Nandita, L., and Devandra, J., Performance of p-Norm Detector in Cognitive Radio Networks with Cooperative Spectrum Sensing in Presence of Malicious Users, *Wireless Communications and Mobile Computing*. Vol. 2017, Article ID 4316029, 8 Pages. DOI:10.1155/2017/4316029, 2017.

[4]. Jayakrsihna, P. S,. Greshma, V., and Sudha,T., Energy Efficient Spectrum Sensing Techniques for Cognitive Radio Networks: A Survey, *International Journal of Computer Applications*, vol. 160, no. 4, pp. 20 – 23, 2017.

[5]. Nelly, R., Bettina, L., Morten, G., Absjorn, M., Carina, G., Helge, B, S, and Jesper, F., Adapted Wavelet Transform Improves Time-Frequency Representations: A Study of Auditory Elicited P300-Like-Evenet-Related Potentials in Rats, *Journal of Neural Engineering*, vol. 14 no. 2, pp. 1 – 8, 2017.

[6]. Wright, A., Walker, J, P., Robertson, D, E., and Pauwels, V., A Comparison of the Discrete Cosine and Wavelet Transforms for Hydrologic Model Input Data Reduction, *Hydrology and Earth System Sciences*, pp. 1 – 23, DOI: 10.5194/hess-2017-26, 2017.

[7]. Yifeng, L., Lihui, Z., Baohui, L., Yan, X., Sanyan, W., Xiaoyang, W., Xiaoyan, L., Rong, L., and Quan, W. (2017). The Simulation Study of three typical time frequency analysis methods, *Bioweb of Conference,* pp. 1 – 7. DOI: 10.1051/bioconf/20170802007, 2017.

[8]. Ruch, D., & Patrick, J., *Wavelet Theory: An Elementary Approach with Applications*. Wiley, New Jersey, 2009.

[9]. Nikookar, H., *Wavelet Radio: Adaptive and Reconfigurable Wireless Systems Based on Wavelets*. Cambridge University Press, Cambridge, 2013.

[10]. Fatima, S., Hassan, E., Naima,K., and Wassim, F. (2015). Matched Filter Detection with Dynamic Threshold for Cognitive Radio Networks, *IEEE International Conference on Wireless Networks and Mobile Communications*, pp. 1 – 6, 2015.

[11]. Daniela, M., and Angel, G., Reducing the Effects of Noise Uncertainty in Energy Detectors for Cognitive Radio Networks, *International Journal of Communication Systems*. pp. 1 – 17, 2017.
[12]. Wilaiporn, L., Kanabadee, S., Kornkamol, T., and Akara, P., Adaptive Two-stage Spectrum Sensing under Noise Uncertainty in Cognitive Radio Networks, *ECTI Transactions on Electrical Eng, Electronics, and Communications*, vol. 14, no.1, pp. 21 – 35, 2016.
[13]. Yuan, L., and Alexandra, D., Channel-Adaptive Spectrum Detection and Sensing Strategy for Cognitive Radio Ad-hoc Networks, *IEEE 10th Conference on Consumer Communications and Networking*, pp. 466 – 471, 2013.
[14]. Galal, E., Detection and Localization of RF Radar Pulses in Severe Noisy Environment using Wavelet Packet Transform Combined with Higher-order Statistics Thresholding Technique, *Progress in Electromagnetics Research* vol. 58, pp. 301 – 317, 2016.
[15]. Mahala, B, V., and Anand, M, J., Adaptive Wavelet Packet Decomposition for Efficient Image Denoising By Using NeighSure Shrink Method, *International Journal of Computer Science and Information Technologies*, vol. 5, no. 4, pp. 5003 – 5009, 2014.
[16]. Elango, S., Thirugnanam, G., and Mangaiyarkarasi, P., Wavelet Packet Based Video Watermarking and Extraction using Independent Component Analysis, *Journal of Advances in Information Technology*, vol. 7, no. 3, pp. 156 – 160, 2016.
[17]. Ilker, B., and Ivan, W, S., On the Dual-Tree Complex Wavelet Packet and M-Band Transforms, *IEEE Transactions on Signal Processing*, vol. 56, no. 6, pp. 2298 – 2310, 2008.
[18]. Li, L., Han, Y., Chen, W., Lv, C., and Sun, D., An Improved Wavelet Packet-Chaos Model for Life Prediction of Space Relays Based on Volterra Series, *PLoS ONE*, vol. 11, no. 6, pp. 1 – 13, 2016.
[19]. Zhinjin, Q., Wang, N., Yue, G., and Laurie, C., Adaptive Threshold for Energy Detector Based on Discrete Wavelet Packet Transform, *Wireless Telecommunications Symposium*, pp. 1 – 5, 2012.
[20]. Wei, N., Chen, Z., and Zhu, A., Research on Adaptive Resolution Spectrum Sensing Method Based on Discrete Wavelet Packet Transform, *Telkomnika Indonesian Journal of Electrical Engineering*, vol. 12, no. 2, pp. 1385 – 1394, 2014.
[21]. Sohail, D. and Saber, E., *Advanced Linear Algebra for Engineers with MATLAB*, CRC Press, Boca Raton, 2009.

[22]. Cooperstein, B., *Advanced Linear Algebra*, 2nd Ed, CRC Press, Boca Raton, 2015.
[23]. Meyer, C, D.,*Matrix Analysis and Applied Linear Algebra*, SIAM, 2000.
[24]. Boyd, S., and Vandenberghe, L., *Convex Optimizatio*n, Cambridge University Press, New York, 2009..

Biographies

Peter Yusuf Dibal is currently a PhD student in communication at the Federal University of Technology Minna. He holds a Masters degree in Electronics and Communications engineering. His research interests are digital signal processing, communications, and VLSI design.

Elizabeth N. Onwuka is a Professor of Telecommunications Engineering. She holds a PhD in Communications and Information Systems Engineering, from Tsinghua University, Beijing, People's Republic of China; a Master of Engineering degree, in Telecommunications; and a Bachelor of Engineering degree from Electrical and Computer Engineering Department, Federal University of Technology (FUT) Minna, Niger State, Nigeria. Her research interest includes Mobile communications network, Mobile IP networks, Handoff management, Paging, Network integration, Resource management in wireless networks, spectrum management, and Big Data Analytics.

Caroline O. Alenoghena holds a PhD in Telecommunications Engineering, and a Masters degree in Electronics Telecommunications. She is a member of the Institute of Electrical and Electronic Engineers MIEEE, Nigerian Society of Engineers (NSE), and Association of Professional Women Engineers of Nigeria APWEN. She is a registered practicing Engineer with the Council for the Regulation of Engineering in Nigeria. Her research interests include intelligent systems and networks.

James Agajo has a PhD in the field of Telecommunication and Computer, Signal Processing. He also has a Master's Degree in Electronic and Telecommunication Engineering. His research interest is in Wireless Sensor Systems, and Network and intelligent system development.